



Strathprints Institutional Repository

Doo, G.H. and Dempster, W.M. and McNaught, J.M. and , DTI (Funder) and , EPSRC (Funder) and , TUVNEL (Funder) and , Hyprotech UK Ltd (now Aspen Technology Inc.) (Funder) (2008) *Improved prediction of shell side heat transfer in horizontal evaporative shell and tube heat exchangers*. Heat Transfer Engineering, 29 (12). pp. 999-1007. ISSN 0145-7632

Strathprints is designed to allow users to access the research output of the University of Strathclyde. Copyright © and Moral Rights for the papers on this site are retained by the individual authors and/or other copyright owners. You may not engage in further distribution of the material for any profitmaking activities or any commercial gain. You may freely distribute both the url (<http://strathprints.strath.ac.uk/>) and the content of this paper for research or study, educational, or not-for-profit purposes without prior permission or charge.

Any correspondence concerning this service should be sent to Strathprints administrator: <mailto:strathprints@strath.ac.uk>

Improved prediction of the heat transfer and pressure drop in evaporative shell side heat exchangers

G.H. Doo¹, W.M. Dempster², J.M. McNaught³

¹ Graham Hart (Process Technology) Limited, Bradford, BD10 8SW, UK

² Department of Mechanical Engineering, University of Strathclyde, Glasgow, G11XJ, UK

³ TUV NEL Ltd, Scottish Enterprise Technology Park, East Kilbride, Glasgow, G75 OQU, UK

Abstract

This paper presents an improved prediction method for the heat transfer and pressure drop in the shell side of an horizontal shell and tube evaporator. The results from an experimental test programme are used in which a wide range of evaporating two-phase shellside flow data was collected from a TEMA E-shell evaporator. The data is compared with shellside heat transfer coefficient and pressure drop models for homogeneous and stratified flow. The comparison suggests deterioration in the heat transfer data at low mass fluxes consistent with a transition from homogeneous to stratified flow. The pressure drop data suggests a stratified flow across the full test range. A new model is presented which suggests the transition in the heat transfer data may be due to the extent of tube wetting in the upper tube bundle. The new model which also takes into account the orientation of the shellside baffles provides a vast improvement on the predictions of the homogenous type models currently used in commercial design software. The new model would enable designers of shellside

evaporators/reboilers to avoid operating conditions where poor heat transfer could be expected and would also enable changes in process conditions to be assessed for their implications on likely heat transfer performance.

1 Introduction

A large number of industrial shell and tube heat exchangers are designed with an evaporating fluid on the shell side. Forced circulation shell side evaporation is generally associated with the design of feed-effluent heat exchangers and reboilers for distillation columns. Good design of a heat exchanger with shell side evaporation involves obtaining a good heat transfer coefficient whilst remaining within the process pressure drop constraints. With shell side two-phase flow, heat transfer performance is strongly linked to the two-phase flow pattern. In order to maintain the boiling process throughout the heat exchanger it is essential that the heat transfer surface remains wetted and that a separation of the liquid and vapour phases does not lead to regions in which the outer surface of the tubes become surrounded by vapour.

Despite the widespread use of heat exchangers with shell side evaporation, there are very few data available in the open literature for boiling two-phase flows on the shellside of real industrial shell and tube heat exchanger geometries. Many of the models and correlations for two-phase pressure drop and flow patterns are based on test data obtained from rectangular tube bundle test sections [1] – [5]. This data can only truly represent the crossflow stream of a real exchanger. Other data from real exchanger geometries with bypass and leakage streams [6] present information for

adiabatic flows of air/water and cannot truly represent the full range of qualities and conditions for a boiling two-phase flow.

As a result, it is common place for the designer of a heat exchanger with shell side evaporation to assume that the liquid and vapour phases are sufficiently well mixed to ensure that the heat transfer surface remains fully wetted and that the nucleate and convective boiling processes can be maintained. However, in practice the flow regime is changing as the liquid evaporates and the distribution of the phases is unclear, particular in the case of industrial scale evaporators. The work presented in this paper attempts to address the effect of flow regimes on the heat transfer and pressure drop performance. Data generated from an HTFS research programme is used to present a model describing a transition in the shell side flow pattern from a homogeneous to a separated/stratified two-phase flow where the heat transfer performance is likely to be poor. These conditions occur primarily at low mass flux where current models have been found to poorly predict the heat transfer suggesting a better performance than actually occurs. The paper describes the experimental data base that the model has been developed from and the evidence which suggests that flow stratification may occur. The model is then developed and performance of the model is assessed by comparison against the data.

2 Test Details

A full description of the test procedures and analysis is given by Doo et al [7] and is only briefly outlined here. Tests were undertaken on an industrial scale shell-and-tube evaporator with three different shell side geometrical configurations. The test

evaporator is a horizontal shell and tube heat exchanger TEMA type AEW unit with a single tube pass. It has 97 tubes with a length of 1240 mm, and the unit is large enough to represent full scale industrial heat exchangers. The principle geometric aspects tested were the orientation of the shellside baffles (vertical or horizontal cut) which control the principal flow direction, the baffle pitch and the inclusion of sealing strips in the crossflow bypass lane. In all tests the evaporating fluid on the shellside was refrigerant R-134A with the fluid on the tubeside being condensing steam. Test ranges and diagrams of the three principal geometries are displayed in Table 1 and Figure 1. The test conditions examined are representative of those found in industrial applications. Each test provides a wide range of mass fluxes ($100\text{-}1000\text{ kg/m}^2\text{s}$) and evaporation conditions (quality ranging from 0.05-0.6) to be investigated. Comparison between Test 1 and 2 allow the effects of baffle orientation to be determined and Test 2 and 3 allow the effect of pitch for a vertical baffle orientation to be investigated.

Data Analysis

The overall heat transfer coefficient for each test run was calculated from the effective heat transfer area and measurements of the steam heat load and the mean temperature difference. The steam heat load was obtained by measuring the steam condensate flow rate at the saturation temperature. The mean temperature difference was based on the saturation temperature of the steam on the tube side and on the R-134A saturation temperature measured at the shell side outlet nozzle (as the liquid at the inlet nozzle may be subject to some sub cooling). The shell side boiling heat transfer coefficient was calculated from this value by subtracting the tube side and tube wall heat transfer resistances from the overall resistance and taking the reciprocal value. The tube side

resistance was estimated based on the predictions of the HTFS shell and tube design program TASC. Uncertainties in the boiling heat transfer coefficient were between 5% and 30% and were generally higher at higher values of the coefficient. Pressure drop measurements were made with the use of two calibrated differential pressure transducers. One of the transducers was connected between the shell side inlet and outlet nozzles and measured the total shell side pressure drop whereas the other was connected between tapping points between the first and last baffle spaces measuring the pressure drop across the baffled region of the shellside. The expanded uncertainty in the measured pressure drop was generally less than 10%

3 Basis of Shellside Models

The calculations for heat transfer and pressure drop in the shellside of a tube and shell heat exchanger are commonly based on a description of the shellside flow first introduced by Tinker [8]. A one dimensional flow network approach is taken where the shellside geometry is divided into a number of flow paths which can be combined to describe the overall shellside flow. This is shown on Figure 2 where the dominant cross flows, bypass flows and additional baffle and tube leakage flows are identified. The mass flows for each path are calculated by knowing the resistance K factors for each path. However, the main assumption made in most models are that during evaporative conditions the flow in each path is a well mixed uniformly distributed two phase flow resulting in the same liquid and vapour distribution in each path. This is the basis of the homogeneous model. However evidence exists, as discussed by Doo et.al. (9) that at a low mass flux conditions a marked drop in heat transfer can be associated with liquid-gas stratification. The experimental data indicates a reduction

in heat transfer for low mass fluxes, as shown in Figure 3, which presents the data for all heat flux conditions tested and indicates that the heat transfer coefficient reduces steadily for mass fluxes below 300 kg/sm^2 . Furthermore, evidence of a sizeable variation in heat transfer over the cross section of the shell side was obtained by plotting tube side outlet temperatures as a ratio of the saturation temperature. Figure 4 shows tube temperature ratios for tubes at low, mid and upper levels in the tube bank and show that while upper levels remain superheated (steam is introduced at superheat) the lower levels are substantially sub-cooled. These results go some way to suggest that the reduction in heat transfer may be associated with stratification of the flow with vapour flow dominating at the top and liquid flow at the bottom. In order to assess this hypothesis a stratified flow model to predict the pressure drop and heat transfer in the shell side has been developed. A homogeneous model has also been constructed which is based on existing methodologies. These two models are then compared against the data obtained from the experimental programme.

Homogeneous Flow Model

The calculation for the flow rate and pressure drop in each flow path is undertaken using correlations for flow path resistance and is based on the assumption that the respective pressure drops in parallel flow paths are equal. The homogeneous flow model created was based on that of the commercial design software HTFS TASC [10]. The model assumes that at a given point along the length of the shell, the vapour quality in each flow path is equal; i.e. the liquid and vapour phases are evenly distributed throughout the flow paths. The pressure drop for this model is calculated from the resolution of the iterative network model of the various flow paths. The shellside heat transfer coefficient is calculated from correlations which describe

nucleate and convective boiling based on the flow rates in each flow path taken from the resolution of the shellside flow model. Pressure loss and heat transfer models are used from well established approaches available in the literature and are described in detail by Doo [7] and also found in [10].

Stratified Flow Model

This homogeneous shellside model was adapted to describe stratified shell side flow. The stratified flow model was based on the assumption that the bottom of the shell is occupied by single phase liquid and the upper section occupied by single phase vapour. The pressure drop model is based on two constraints.

The first is that (as in the homogeneous model) pressure drops in parallel flow paths are equal and the second that the pressure drops in the liquid and vapour phases are equal. It is also assumed that interface shear between the liquid and vapour phases is negligible.

The pressure drop was then calculated using the following procedure:

- Estimate the shellside void fraction
- Calculate modified flow path areas based on the area covered by the liquid/vapour phase
- Calculate the pressure drop in each phase based on the new flow areas and the shellside flow network model.
- If the phase pressure drops are equal the calculation is resolved, if not then the void fraction is re-estimated and the procedure repeated.

The shell side heat transfer coefficient for the stratified flow model requires to be consistent with the calculation of the heat transfer between the shell and tube flows. The stratified model maintains consistency with the network approach and calculates the heat transfer between the shell and tube streams using a local overall heat transfer coefficient, U as expressed in equation 1. The first term on the RHS represents the shell side convection heat transfer and the other terms, the shell side fouling, tube wall conduction, tube side convective heat transfer and fouling respectively.

$$\frac{1}{U} = \frac{1}{\alpha_s} + r_s + \frac{y_d}{\lambda_w} \frac{d_o}{d_w} + \left(\frac{1}{\alpha_t} + r_t \right) \frac{d_o}{d_t} \quad (1)$$

In the stratified model the shell side heat transfer is calculated by a void fraction weighted combination of the nucleate/convective boiling coefficient for the liquid pool and the single phase vapour coefficient for the upper section of the evaporator, as indicated in equation (2)

$$\alpha_s = \varepsilon_g \alpha_g + (1 - \varepsilon_g) \alpha_{boiling} \quad (2)$$

Where ε_g is the void fraction obtained from the iterative shell side flow network pressure drop model and α_g and $\alpha_{boiling}$ are the vapour phase and boiling heat transfer coefficients respectively, established from the correlations used in the homogeneous model.

4 Results :Heat Transfer

To examine the homogenous and stratified flow models comparisons were made with the experimental heat transfer data for the three test geometries and are presented in Figure 5. From the comparisons of Figure 5 it can be seen that for all three test conditions the homogenous model gives reasonable predictions of the heat transfer coefficient in the higher mass flux range (300-600 kg/m²s) and over predicts by up to six times the experimental values in the lower range (100-300 kg/m²s). In contrast the stratified flow model predicts the data more accurately at the low mass fluxes for all test conditions where the smaller heat transfer coefficients have been obtained. At higher mass fluxes the stratified model under predicts the heat transfer coefficient by up to a factor of two. This is consistent with the argument that a change to a stratified flow pattern could be causing deterioration in the heat transfer coefficient in this range. The stratified flow pattern would lead to vapour blanketing around some of the upper rows in the tube bundle and cause a decrease in the heat transfer coefficient due to the fact that the normal boiling mechanisms cannot be maintained in this area. At the higher mass fluxes in Figure 5 the heat transfer coefficient is better represented by the homogeneous model.

Current models based on homogeneous assumptions result in substantial over prediction of the heat transfer and give a false impression of a viable heat exchanger design. Thus substantial benefit can be gained by predicting the heat transfer in regions of poor heat transfer. The results shown here suggest that the greatest benefit would be obtained from a model that could predict the onset of the stratified flow regime and which could be used to prevent operation with this type of flow. The development of such a model is discussed below.

5 Proposed Model (Heat Transfer)

An assessment of the open literature revealed that there was very little information on the subject of flow pattern transitions in two-phase shellside flow. The only available shellside maps were based on very limited air/water tests in ideal geometries. In addition the transitions are described in terms of dimensionless groups which are empirically correlated to experimental data. There is far more information on the subject of flow pattern transition in tubeside flow, which is in turn based on a far larger range of experimental data. The shellside maps of Grant [11] gave a reasonably good representation of the transition in the experimental data. However due to the limited data on which these flow pattern maps are based and also in the inherent limitations due to the empirical nature of the model, it was decided to use the more established and better understood tube based flow regime models to describe the transition.

Various tube geometry models were examined to provide a theoretical basis for describing the flow pattern transition to stratified flow in the shell side geometry [12] – [14]. From this review, the Taitel and Dukler method [14] proved to give the best agreement with the experimental data and also had a theoretical basis from which a shellside flow model could be developed. The authors base the model on the idea that an increase in the gas velocity over the stratified liquid surface will eventually cause a wave large enough to form a blockage in the pipe causing the onset of intermittent flow. The model begins by considering a stratified flow with a wave existing on the surface over which the gas flows, as shown in Figure 6. When a critical gas velocity is

reached there is a transition from stratified to intermittent flow in the tubes. This critical velocity is calculated using equation 3

$$u_{g(Crit)} = C_2 \left[\frac{(\rho_l - \rho_g) g_n A_g}{\rho_g \frac{dA_l}{dh_l}} \right]^{1/2} \quad (3)$$

Where A_g is the cross sectional flow area of the vapour in the stratified flow without the wave, A_l and h_l are the corresponding liquid phase area and height, g_n is the acceleration due to gravity and C_2 is given by:

$$C_2 = 1 - \frac{h_L}{D} \quad (4)$$

D is the diameter of the tube corresponding with the liquid height h_l . A superficial gas velocity value higher than that predicted by equation 2 would cause a departure from stratified flow.

The assumption made on applying this type of transition to the shellside is that the velocity high enough to cause a departure from stratified flow in the tubeside case would be high enough to cause a transition from stratified flow in the shellside case. Although the Taitel/Dukler model describes the transition from stratified flow to intermittent flow in tubes, it is assumed in the shellside case that the transition represents a departure from stratified flow to a regime where there is sufficient tube wetting in the upper bundle for the application of the homogeneous boiling heat

transfer model. This argument would seem inherently more applicable to the shellside geometry when the baffle cut orientation is vertical as opposed to horizontal. With a vertical baffle cut the stratified flow pattern would be similar to that shown in Figure 7, whereas with the horizontal baffle cut it is more likely to be similar to that shown in Figure 8.

In fact the heat transfer data from the experimental tests suggested there may be a more gradual transition in the two-phase flow pattern with the horizontal baffle cut. This may be explained by the fact that horizontal baffles which force up-and-over flow hinder the process of stratification and maintain tube wetting of the upper tube rows over a wider mass flux range.

To assess how the model of Taitel and Dukler compares with the shellside data it was essential to generate predictions of the critical gas velocity from equation 3 for the shellside case. The superficial gas velocity of a particular flow can be determined from equation 5.

$$u_{sg} = \frac{\dot{m}x}{\rho_g} \quad (5)$$

For shellside flow, the mass flux \dot{m} is based on the minimum-crossflow and bypass areas and x is the vapour mass quality. The value of u_{sg} obtained from equation 5 is compared with the value for the critical vapour phase velocity from equation 3.

Calculation of the critical vapour phase velocity requires calculation of the parameters C_2 , A_g and $\frac{dA_l}{dh_l}$ which are all functions of the shellside void fraction ε_g . The void

fraction used is calculated by running the stratified flow model at the given conditions of mass flow rate and vapour quality. In the tubeside model a value of $u_{sg} > u_{g(Crit)}$

would imply a transition from stratified to intermittent flow. As some of the data suggested a more gradual transition it was decided to create a model which would be able to describe the process of wetting an increasing fraction of the tubes in the upper tube bundle. A wetting factor was introduced that describes the fraction of the tubes in the upper bundle that are surrounded by liquid. A value of $W = 0$ implies that the flow is completely stratified as in Figure 9(a) with no wetting of the upper tube bundle, whereas $W = 1$ implies that all of the tubes in the upper bundle are surrounded by a dispersed liquid flow, as shown in Figure 9(b).

Equations 6 – 8 were used to control the range of gas superficial velocities over which the transition from no tube wetting in the upper bundle to complete tube wetting occurs.

$$\text{If } u_{sg} < b_1 u_{g(Crit)} \quad \text{Then } W = 0 \quad (6)$$

$$\text{If } u_{sg} > b_2 u_{g(Crit)} \quad \text{Then } W = 1 \quad (7)$$

$$\text{If } b_1 u_{g(Crit)} < u_{sg} < b_2 u_{g(Crit)} \quad \text{Then } W = \left(\frac{\frac{u_{sg}}{u_{g(Crit)}} - b_1}{b_2 - b_1} \right) \quad (8)$$

b_1 and b_2 are factors to determine the lower and upper critical velocity boundaries between the homogeneous and stratified conditions. These must be chosen to define the range of critical velocities over which the flow regime change occurs, but also reflect inadequacies in using the Taitel and Dukler approach. The equation for W in (8) represents a linear interpolation of tube wetting due to liquid entrainment in the

Improved prediction of the heat transfer and pressure drop in evaporative shell side heat exchangers 13

vapour phase between the lower and upper boundary conditions. These factors have been determined by comparison of the model predictions with the experimental test data. It has been found that the most appropriate values are influenced by the orientation of the baffles indicating an effect on the flow regime of the baffle arrangement. The values to give the best agreement with the results for the horizontal baffle cut (Test 1 data) are shown in (9). Whereas with the vertical baffle cut (Test 2 and Test 3 data) the factors shown in (10) gave the best result.

$$\text{Horizontal baffles } b_1 = 0.25 \text{ and } b_2 = 1.75 \quad (9)$$

$$\text{Vertical baffles } b_1 = 0.75 \text{ and } b_2 = 1.25 \quad (10)$$

Figure 10 shows a comparison of the heat transfer coefficient predicted using the transition model compared with the experimental data and predictions using the homogeneous heat transfer model. It can be seen that the new model is a vast improvement on the predictions of the homogeneous type model at the low mass flux range. In all three test geometries, the introduction of the transition model vastly improves the prediction of the experimental data. Using this heat transfer model would prevent the design of heat exchangers being undersized when based on current methods, which predict an over optimistic heat transfer coefficient. In addition the model would be able to more accurately predict the performance of an existing heat exchanger when there is a change in process or operating conditions. A disadvantage is that the flow regime transition has been established semi-empirically from the test data and therefore could limit the generality of the model. However, the test data reflects realistic conditions encountered in industrial sized heat exchangers which gives confidence on the generality of the predictions.

Pressure Drop

Figure 11 below shows the experimental data plotted against the predictions of the stratified flow and homogeneous flow pressure drop models for each test. Over the whole range of test data it appears that the best comparison with experimental results is achieved using the stratified flow model. One proposed explanation for this would be that the flow is predominantly stratified over the full range but with entrainment of liquid at higher mass fluxes. In this case, the transition in the heat transfer data represents a point at which there is sufficient entrainment of liquid in the vapour phase to maintain the boiling process in the upper tube rows (Similar to the arrangement displayed in Figure 9(b)). In this case the pressure drop would be largely unaffected by the transition whereas the heat transfer coefficient would be vastly improved. At this stage improvement in model development would be enhanced by visualisation of the flow regime conditions occurring in the shell side. This would enable a better insight into the physical mechanisms that cause the transition in flow pattern and lead to a deterioration in heat transfer performance.

The overall accuracy of the heat transfer and pressure drop predictions is shown on Figure 12(a) and 12(b), where a direct comparison between prediction and experimental values are made for Tests 1, 2 and 3. The heat transfer predictions can be achieved to an RMS average accuracy of +/- 26%, while the pressure drop can be achieved to an RMS average of 30%. The general spread of errors is seen in the graphs where an over prediction of the heat transfer coefficient is apparent at lower

values and a slight under prediction at higher values. The pressure drop is moderately over predicted over the whole range.

6 Conclusions

A shellside model has been created which accounts for a complete stratification of the liquid and vapour phases. The model utilises the Taitel and Dukler model for the transition from stratified to intermittent flow. The nature of the flow pattern transition on the shellside appears to be related to the orientation of the baffle cut. The horizontal baffle cut giving a more gradual transition to stratified flow.

The new model provides significant improvements in the predictions of both heat transfer coefficient and pressure drop when compared with the shellside evaporation test data. It accounts for the affects of a transition to a gravity separation of the liquid and vapour phases and would prevent designers from producing heat exchangers with insufficient area when a stratified flow pattern is likely. The model could also be used to assess the implications of changing operating conditions on the likely heat transfer performance of an existing evaporator.

Nomenclature

A_g	Cross sectional area covered by gas/vapour phase in stratified flow (m ²)
A_l	Cross sectional area covered by liquid phase in stratified flow (m ²)
C_2	Parameter defined in equation (3)
D	Tube or shell internal diameter (m)
g_n	Acceleration due to gravity (m/s ²)
h_l	Height of liquid/vapour interface in stratified flow (m)
g_n	Acceleration due to gravity (m/s ²)
Low_{bc}	Lower boundary condition in transition region of new model
\dot{m}	Total flow mass flux / mass velocity (kg/m ² s)
N	number of experimental data points
RMS	Root Mean Square average = $\sqrt{\frac{1}{N} \left(\frac{predicted - experimental}{predicted} \right)^2}$
r_b, r_w	tube and wall fouling resistance (m ² K/W)
$u_{g(Crit)}$	Critical gas velocity in transition equation (2)
Up_{bc}	Upper boundary condition in transition region of new model
u_{sg}	Superficial gas phase velocity (m/s)
y	wall thickness (m)
W	Tube wetting parameter in new transition model
x	Vapour mass fraction / quality
$\alpha_{boiling}$	Heat transfer coefficient from homogeneous shellside model (W/m ² K)
α_g	Vapour phase heat transfer coefficient in stratified flow (W/m ² K)

- α_s Shell side heat transfer coefficient (W/m²K)
- $\alpha_{stratified}$ Heat transfer coefficient from stratified shellside model (W/m²K)
- α_t tube side heat transfer coefficient (W/m²K)
- λ_w tube wall thermal conductivity (W/mK)
-
- ε_g Void fraction in stratified flow
- ρ_g Vapour/gas density (kg/m³)
- ρ_l Liquid phase density (kg/m³)

References

- [1] Dowlati, R, Chan, A.M.C; Kawaji, M. , Hydrodynamics of Two-Phase Flow Across Horizontal In-Line and Staggered Tube Bundles, Transactions of the ASME, Journal of Fluids Engineering, Vol.114, p450-456, Sept. 1992. (article)
- [2] Dowlati, R, Kawaji, M; Chan, A.M.C , Two-Phase Crossflow and Boiling Heat Transfer in Horizontal Tube Bundles, ASME, Journal of Heat Transfer, Vol.118, p124-131, Feb. 1996. (article)
- [3] Grant, I.D.R. and Murray, I., Pressure Drop on the Shell-side of a Segmentally Baffled Shell-and-Tube Heat Exchanger with Horizontal Two-Phase Flows, NEL report 560, 1974. (unpublished report)

- [4] Grant, I.D.R.; Chisholm, D.; Cotchin, C.D., Shellside flow in horizontal condensers, Paper 80-HT-56, Joint ASME, AIChE National Heat Transfer Conference, Orlando, Florida, 1980. (proceedings)
- [5] Xu, G.P; Tou, K.W; Tso, C.P., Two-Phase Void Fraction and Pressure Drop in Horizontal Crossflow across a Tube Bundle, ASME, Journal of Heat Transfer, Vol.120, p140-145, March 1998. (article)
- [6] Grant, I.D.R.; Cotchin, C.D.; Henry, J.A.R. , Submergence in baffled shell-and-tube heat exchangers, First UK National Conference on Heat Transfer, Institution of Chemical Engineers, Symposium Series No.86, Vol.1, pp 673-683, (1984). (proceedings)
- [7] Doo G. A modelling and experimental study of evaporating two phase flow on the shell side of shell and tube heat exchangers, PhD Thesis, University of Strathclyde, Glasgow UK, 2005. (thesis)
- [8] Tinker, T.S., Shell side characteristics of shell and tube heat exchangers – A simplified rating system for commercial heat exchangers, Trans. of the ASME, Vol.80 (1), p36-49,1955. (article)
- [9] Doo, G., McNaught, J.M., Dempster, W.M., Shellside evaporation in a TEMA E-Shell: Flow patterns and transitions, Applied Thermal Engineering, Vol.24, pp1195-1205 (2004). (article)

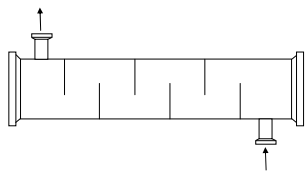
[10] HTFS Design Report 12, TASC 3, Shell and Tube Heat exchanger program, HTFS, 1988. (unpublished report)

[11] Grant, I.D.R, Cotchin, C.D, White, Two-phase up-and-down flow on the shellside of a baffled shell-and-tube heat exchanger', HTFS RS report, RS742, 1987. (unpublished report)

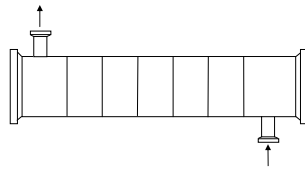
[12] Chen, X.T., Cai, X.D., Brill, J.P., A general model for transition to dispersed bubble flow', Chemical Engineering Science, Vol. 52, (23) pp 4373 – 4380, 1997. (article)

[13] Weisman, J., Duncan. D. Gibson. J., Crawford, T. , Effects of fluid properties and pipe diameter on two-phase flow patterns in horizontal lines, Int. Journal of Multiphase Flow, Vol.5, pp 437 – 462. (article)

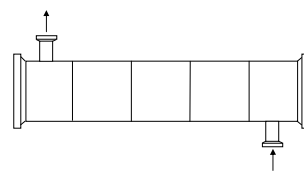
[14] Taitel, Y.; Dukler, A.E., A model for predicting flow regime transitions in horizontal and near horizontal gas-liquid flow, AIChE Journal, Vol. 22, (1) pp 47-55, 1976. (article)



Test 1 – horizontal baffle



Test 2 – vertical baffle cut



Test 3 – vertical baffle cut increased pitch

Figure 1- Baffle arrangements for different test geometries

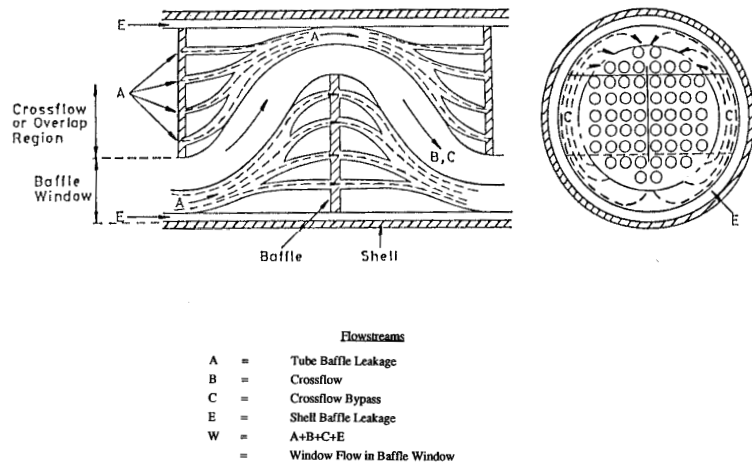


Figure 2 – Shellside flow network proposed by Tinker [8]

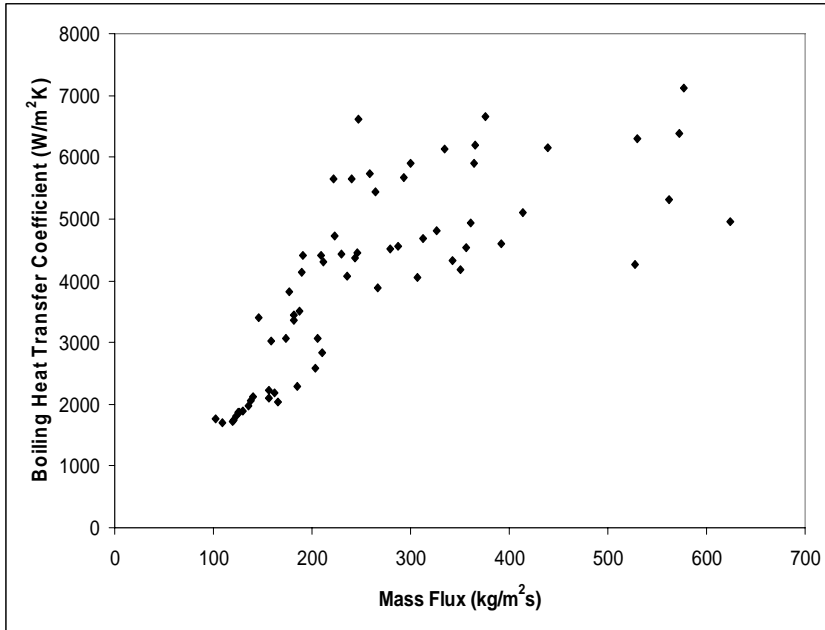


Figure 3 Plot of heat transfer coefficient versus mass flux for various heat fluxes (18-49 kW/m²)

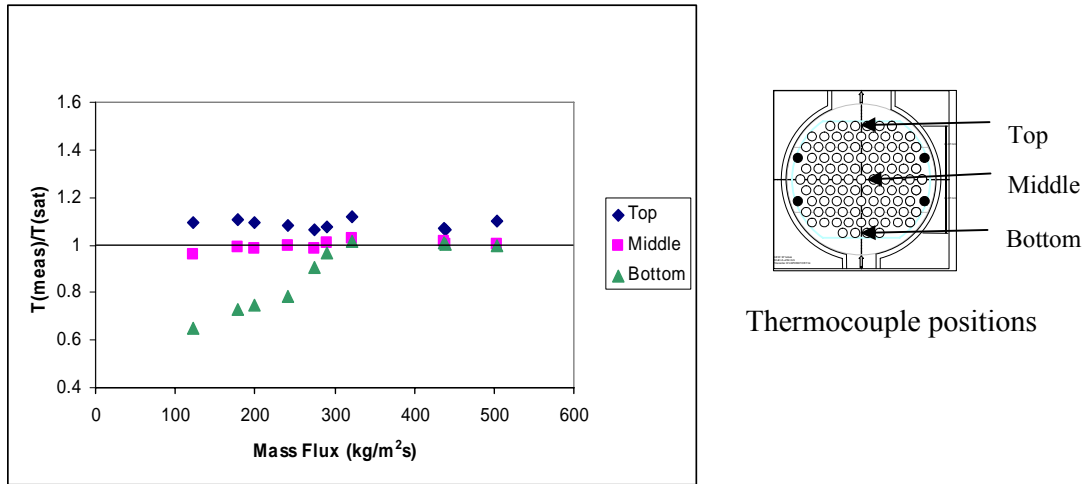
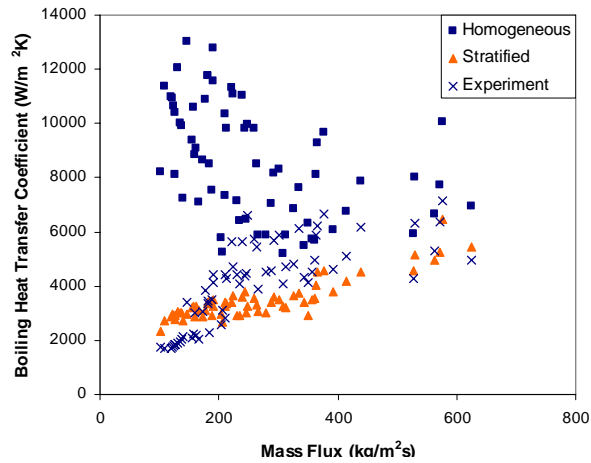
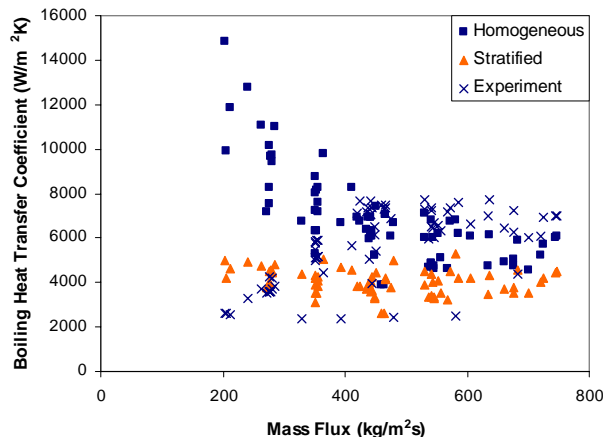


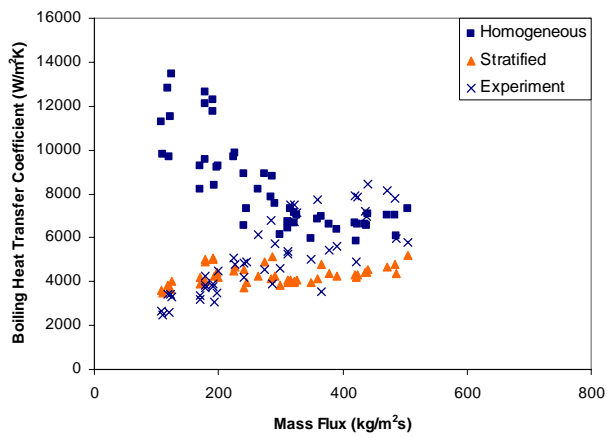
Figure 4 Measured to Saturated Temperature Ratio vs. Mass flux for tubeside thermocouples in Test 3, (Heat Flux= 34 kW/m^2)



Test 1: horizontal baffle cut



Test 2: vertical baffle cut



Test 3: vertical baffle cut, increased pitch

Figure 5 – Boiling heat transfer coefficient data and model predictions

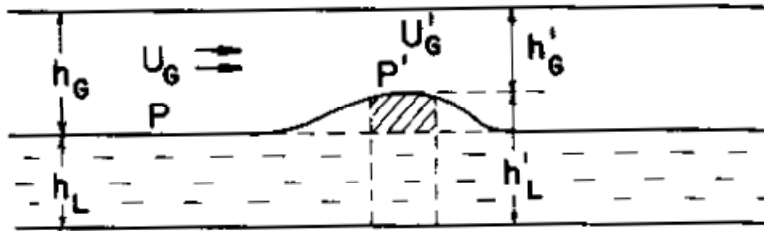


Figure 6 – Instability for a solitary wave [14]

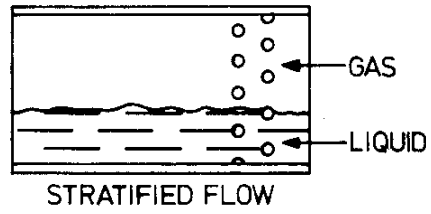


Figure 7 – Stratified shellside flow for vertical baffle cut

A Tube-baffle leakage flow
E Baffle-shell leakage flow
C Bundle-shell bypass flow

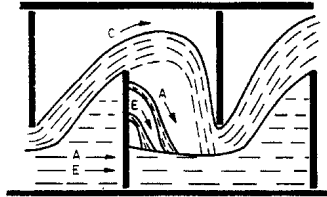
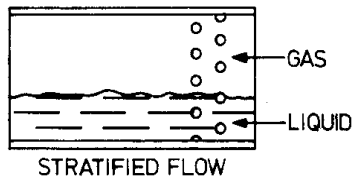
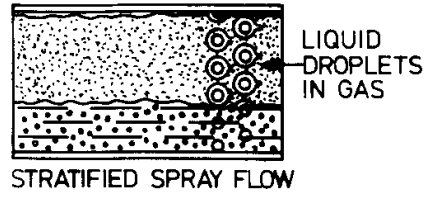


Figure 8 - Stratified Flow in Horizontal Baffle-Orientation [11]



(a) – Completely stratified



(b) – Flow with liquid entrainment

Figure 9 – Completely Stratified flow and Stratified flow with liquid entrainment

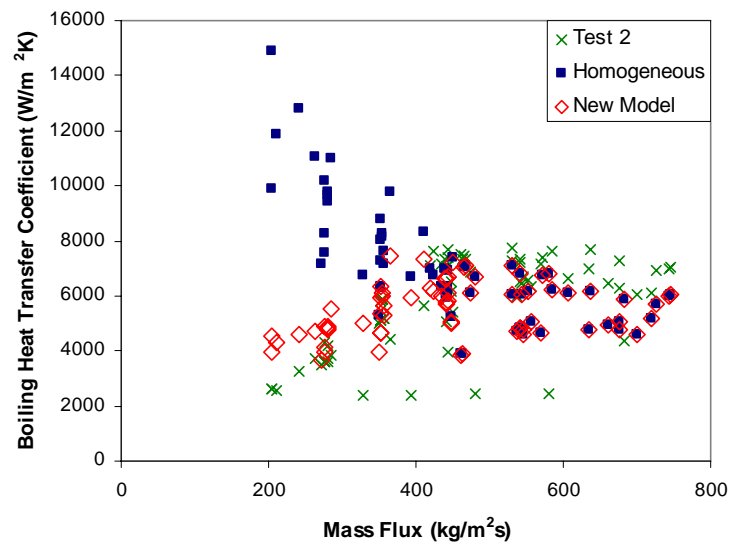
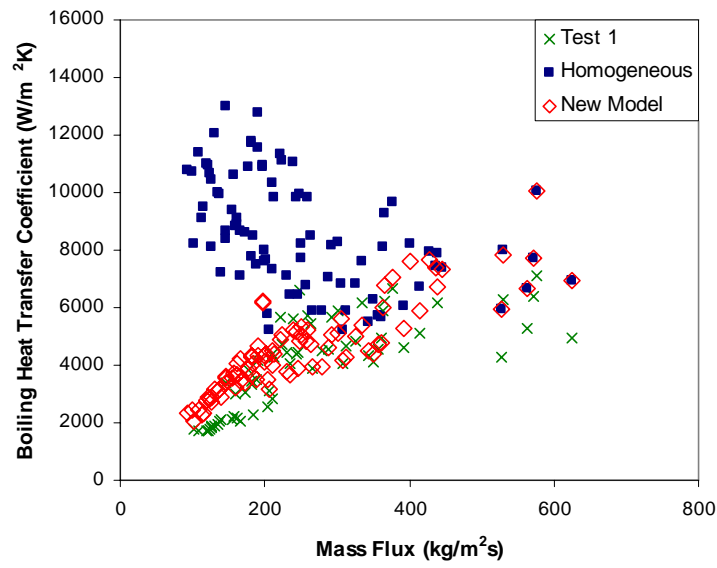
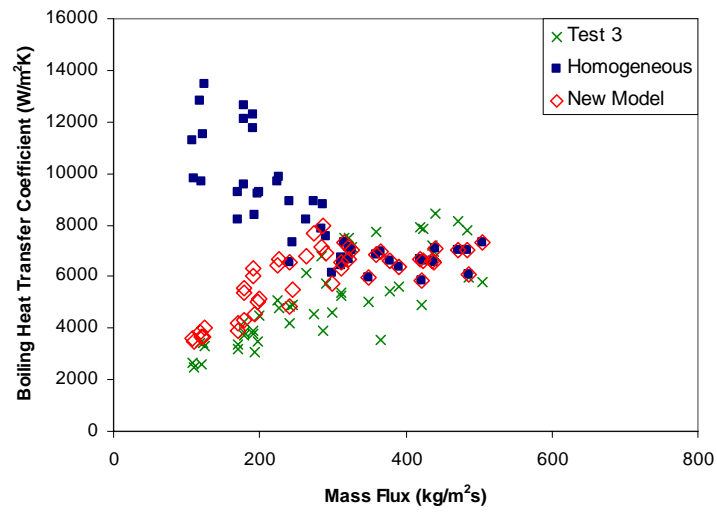
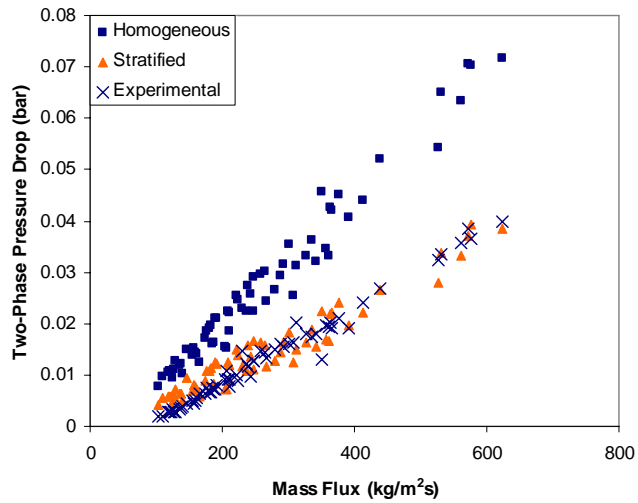
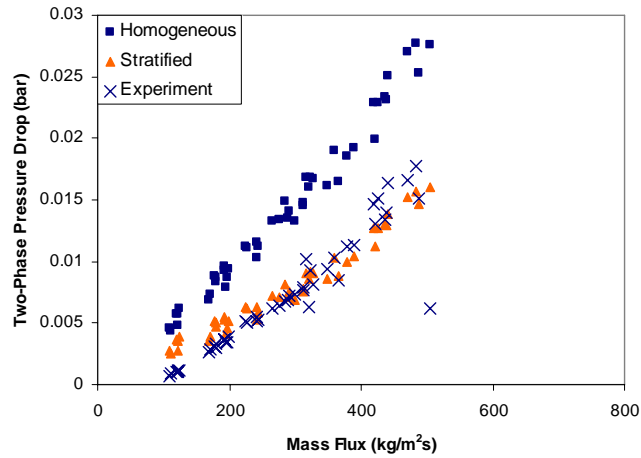


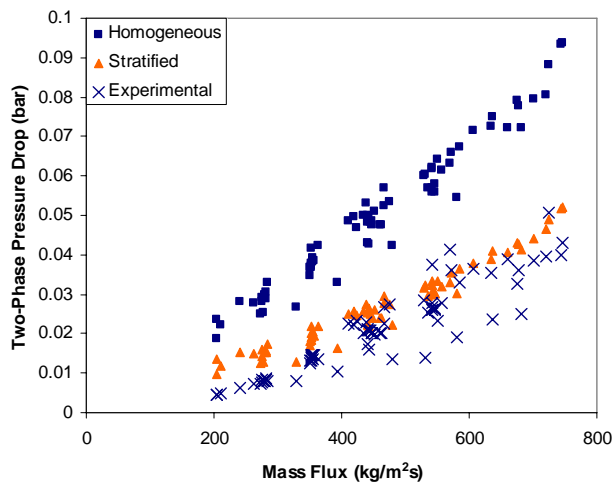
Figure 10 – Comparison of new heat transfer model with widely used homogeneous model.



Test 1

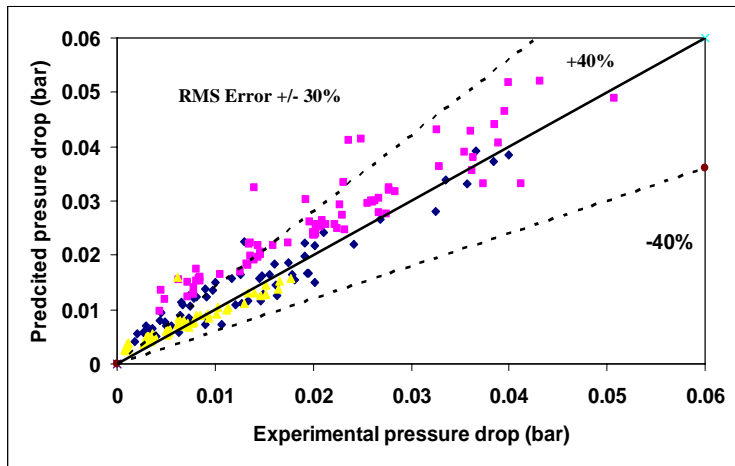


Test 2

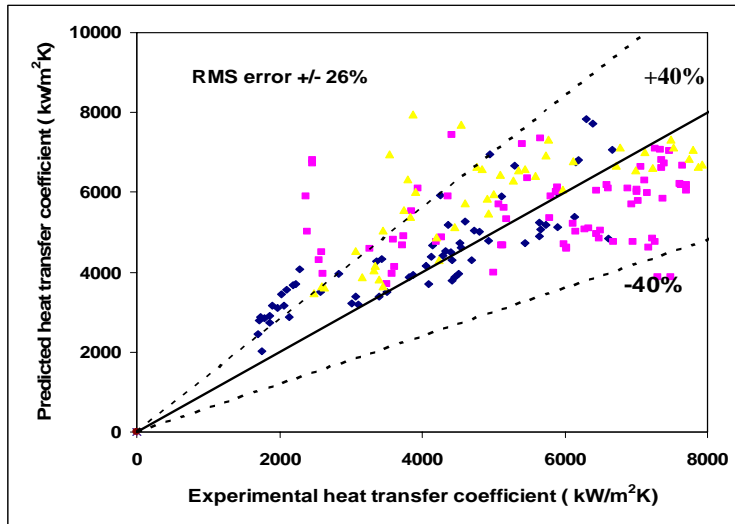


Test 3

Figure 11 – Comparisons of two-phase pressure drop data with shellside models



(a) Pressure drop



(b) Heat transfer coefficient

Figure 12 Comparison between predicted and experimental values

	TEST 1	TEST 2	TEST 3
Heat load (kW)	108-255	120-220	146-230
Mean Tem Difference (K)	7.4-16.4	5.5-16.7	7.5-15
R-134A inlet pressure (bar)	5.8-9.3	5.6-8.13	6.43-7.39
Steam inlet pressure (bar)	0.041-0.101	0.038-0.094	0.048-0.087
R-134A mass Flux (kg/m ² s)	140-856	162-1023	108-504
Heat Flux (kW/m ²)	19-44	24-37	26-37
Baffle pitch (mm)	156	156	260
Baffle orientation	horizontal	vertical	vertical
Sealing strips in Bypass	yes	yes	no
Outlet vapour quality	0.11-0.68	0.09-0.5	0.11-0.56
Recirculation Ratio	0.47-8.1	1-10.1	0.79-8.1

Table 1 Test conditions for experimental tests